

Four-wave scattering of light by coherently excited polaritons

G Kh Kitaeva, K A Kuznetsov, A A Mikhailovskii ¶,
I I Naumova, A N Penin

Abstract. An analysis was made of four-wave scattering of light by coherently excited phonon polaritons in homogeneous LiIO_3 and Mg:LiNbO_3 crystals, and also in periodically poled Nd:Mg:LiNbO_3 . An investigation of lithium niobate crystals revealed a considerable discrepancy between the theoretically predicted and the experimentally determined dependences of the Stokes component intensity on the polariton phase mismatch. General expressions were derived for the line profile of the four-wave scattering in crystals with a periodic distribution of their nonlinear optical properties and in spatially confined nonlinear regions.

1. Introduction

Phonon polariton spectroscopy is extremely sensitive to the state of the investigated medium. Low-dimensional effects, small variations of the composition of a crystal, and the crystal lattice symmetry influence the dispersion relationships of polaritons. If the phonon frequencies and their damping constants remain constant, but the oscillator strengths vary, Raman scattering spectroscopy generally fails to provide information on possible changes in the state of the investigated object. On the other hand, polariton spectroscopy methods make it possible to investigate these changes because the overall nature of the polariton dispersion curves becomes distorted.

Spontaneous three-wave parametric scattering of light by polaritons, observed at low angles, is currently being used successfully to study crystals without inversion symmetry [1]. However, the range of application of this method is greatly limited because, as a result of the relatively low intensity of the signal wave, it is possible to investigate only the characteristics averaged over fairly extended regions of the scattering medium. A study of polaritons in low-dimensional spatially inhomogeneous crystalline structures requires the use of high-sensitivity low-noise detectors with a long accumulation

time. The task of increasing further the spatial resolution may be tackled by active spectroscopy of nondegenerate four-wave mixing of optical waves.

In a medium which does not have an inversion symmetry it is possible to excite simultaneously direct coherent four-wave scattering as well as cascade coherent scattering of light, which essentially represents two consecutive processes of parametric frequency conversion. The direct scattering efficiency is proportional to the cubic nonlinearity of the medium $\chi^{(3)}$ and the cascade scattering efficiency is proportional to the product of two effective quadratic nonlinearities $\chi^{(2)}$. If an excited intermediate state is in resonance with a phonon polariton and the dispersion characteristics of all other waves are known, cascade scattering can be used to investigate the polariton state.

In the first stage of this cascade scattering process, two pump waves of frequencies ω_1 and ω_2 ('heating' waves) excite a polariton state of frequency ω_p , which is equal to the difference between the pump wave frequencies:

$$\omega_p = \omega_1 - \omega_2 . \quad (1)$$

In the second stage a third (probe) pump wave of frequency ω_L is scattered by the excited polariton wave. The Stokes component of the scattered radiation is then recorded and its frequency is

$$\omega_s = \omega_L - \omega_p . \quad (2)$$

The phase-matching conditions for these two processes are as follows:

$$\tau_1 \equiv (\mathbf{k}_1 - \mathbf{k}_2) - \mathbf{k}_p = 0 , \quad (3)$$

$$\tau_2 \equiv (\mathbf{k}_L - \mathbf{k}_p) - \mathbf{k}_s = 0 , \quad (4)$$

where \mathbf{k}_i are the wave vectors of the interacting waves; τ_1 and τ_2 are the values of the phase mismatch. The frequency- and phase-matching conditions for direct four-wave scattering can be written as follows:

$$\omega_s = \omega_L - (\omega_1 - \omega_2) , \quad (5)$$

$$\Delta\mathbf{k} \equiv \mathbf{k}_L - \mathbf{k}_s - \mathbf{k}_1 + \mathbf{k}_2 \equiv \tau_2 - \tau_1 = 0 . \quad (6)$$

The first investigations of four-wave scattering of light by polaritons in media without a centre of inversion appeared in the mid-1960s [2]. The later investigations [3–7] were concerned mainly with an analysis of the interference between direct and cascade processes, and with the dispersion of the cubic susceptibility $\chi^{(3)}$. Cascade four-wave scattering of light is nowadays used successfully in studies of polariton states by time- and space-resolved spectroscopy [8, 9]. We shall consider steady-state frequency – angular polariton spectroscopy [10]. In accordance with the generally accepted model, developed

¶ This author's name is sometimes spelt Mikhailovsky in the Western literature.

G Kh Kitaeva, K A Kuznetsov, A A Mikhailovskii, I I Naumova, A N Penin
Physics Department, M V Lomonosov Moscow State University,
Vorob'evy gory, 119899 Moscow, Russia
tel. (007) (095) 939 43 72; e-mail: postmast@qopt.ilc.msu.su

in Refs [3–7], the frequency – angular distribution of the scattered radiation intensity should be related directly to the dispersion characteristics of polaritons. However, in all the theoretical investigations published so far the scattering medium has been regarded as homogeneous and fairly extended, so as to satisfy the condition that the linear size of the scattering object l is much greater than the mean free path $1/\alpha_p$ of a polariton:

$$l\alpha_p \gg 1, \quad (7)$$

where α_p is the absorption coefficient of a polariton wave. Moreover, the scattering element is assumed to be an infinite planar layer. According to this model, the scattered-radiation intensity depends on the wave mismatch as follows [7]:

$$I_s \propto \text{sinc}^2\left(\frac{\Delta k l}{2}\right) \left[\beta^2 + \frac{2\beta\tau_1}{(\alpha_p/2)^2 + \tau_1^2} + \frac{1}{(\alpha_p/2)^2 + \tau_1^2} \right], \quad (8)$$

where

$$\beta \equiv \frac{n_p c \cos \theta_p}{2\pi\omega_p} \frac{\chi^{(3)}}{\chi_1^{(2)}\chi_2^{(2)}} \quad (9)$$

is the ratio of the contributions of the direct and cascade processes to the scattered-radiation intensity; θ_p is the angle governing the orientation of a wave vector in a crystal; $\chi_1^{(2)}$ and $\chi_2^{(2)}$ are the effective quadratic susceptibilities for the first and second stages of the cascade scattering process; $\chi^{(3)}$ is the effective cubic susceptibility for the direct process; n_p is the refractive index for a polariton wave; c is the velocity of light in vacuum. In expression (8) the first term in square brackets describes the direct four-wave interaction and the last term, the pure cascade scattering; the middle term represents interference between the direct and cascade processes.

Our task will be to compare the results of an experimental determination of the polariton parameters by this and other well-known methods in the specific case of lithium iodate crystals and of lithium niobate crystals doped in various ways, and to consider the feasibility of extension of this method to various classes of inhomogeneous media including spatially confined structures and crystals with small-scale inhomogeneities.

2. Four-wave scattering of light in homogeneous crystals

The dispersion properties of polaritons in homogeneous LiIO_3 crystals (investigated by us in the frequency range 620–760 cm^{-1}) and in $\text{Mg}:\text{LiNbO}_3$ crystals (500–560 cm^{-1}) were first determined by the method of three-wave spontaneous scattering of light [11]. The dispersion of the refractive index in the range of the frequencies of the remaining waves was determined, for $\text{Mg}:\text{LiNbO}_3$ crystals with various concentrations of Mg, by the prism method and the data for LiIO_3 were taken from Ref. [12].

Experimental observations of four-wave coherent scattering of light were made by using apparatus the basic setup of which was described in Ref. [10]. We employed the Stokes analogue of the CARS spectroscopy, which enabled us to record the three-wave spontaneous scattering spectra in the absence of polariton-‘heating’ pumps without any additional change in the detection scheme. The ‘heating’ pumps were

radiations from an Nd:YAG laser (pulse duration 20 ns) and from a frequency-tunable $\text{LiF}:F_2^-$ laser. The probe pump was the second harmonic of an Nd:YAG laser.

In accordance with the theoretical model, information on the polariton characteristics can be obtained at any fixed frequency from the dependence of the scattered-radiation intensity $I_s(\tau_1)$ on the polariton phase mismatch τ_1 (provided the phase-matching condition $\Delta k = 0$ is satisfied by the direct scattering process). Therefore, the following procedure was adopted in determination of the polariton characteristics:

(1) At each polariton frequency we selected the appropriate tunable-laser frequency ω_2 and recorded the signal radiation at the frequency ω_s , in accordance with conditions (1) and (2).

(2) We determined the two-dimensional distribution of the signal wave intensity as a function of two variable parameters (Fig. 1). The first parameter was the angle α between the probe pump beam and the optic axis of the crystal, whereas the second parameter was the angle of incidence θ_1 of one of the ‘heating’ pumps on the crystal.

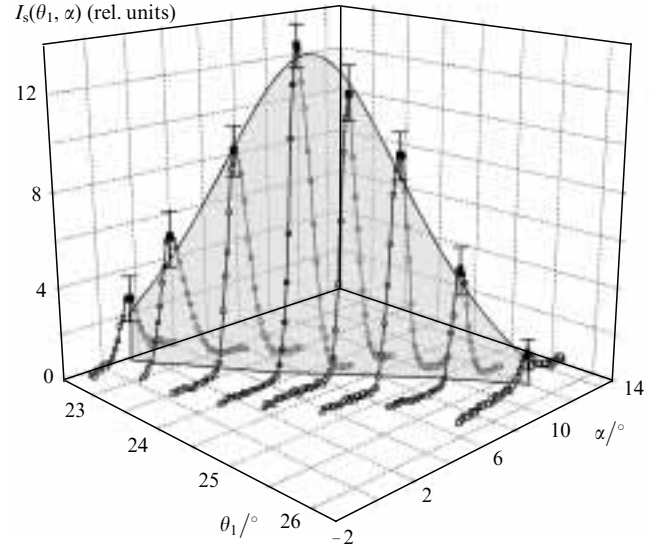


Figure 1. Section of a two-dimensional distribution $I_s(\theta_1, \alpha)$ by a surface $\alpha(\theta_1)$, corresponding to the condition $\Delta k(\theta_1, \alpha) = 0$.

(3) We determined the curve representing intersection of the two-dimensional distribution $I_s(\theta_1, \alpha)$ by a surface defined by the condition of exact phase matching for the direct four-wave process, i.e. the condition $\Delta k(\theta_1, \alpha) = 0$. Following this algorithm, we determined the dependence $I_s(\tau_1)$.

In all the experiments we found that the dependences $I_s(\tau_1)$ had practically no ‘background’ associated with the direct processes. This was evidence of the relative smallness of the components of the effective cubic nonlinear susceptibility.

In accordance with the cascade scattering model, in this case the dependence $I_s(\tau_1)$ has the form of the Lorentz function. Determination of the maximum of $I_s(\tau_1)$ makes it possible to find the refractive index, as well as the real parts of the permittivity and the polariton wave vector. The absorption coefficient of a polariton wave and also the imaginary parts of the permittivity and of the wave vector are deduced from the half-width of $I_s(\tau_1)$.

Figs 2a and 2b give our experimental dependences $I_s(\tau_1)$ and the results of their approximation for LiIO_3 ($\omega = 741 \text{ cm}^{-1}$) and $\text{Mg}:\text{LiNbO}_3$ ($\omega_p = 541 \text{ cm}^{-1}$, 4.2% molar concentration of MgO) crystals. The approximation was made, starting from the expected Lorentzian profile of $I_s(\tau_1)$, by selection of the polariton parameters. In these calculations we took into account the real angular divergences and frequency widths of all the pumps, leading to an additional broadening of the experimentally determined $I_s(\tau_1)$ curves. All the results of our determination of the real and imaginary parts of the permittivity and of the polariton wave vector, made for an LiIO_3 crystal, were in good agreement with the results obtained by the three-wave spontaneous scattering method.

However, in the case of $\text{Mg}:\text{LiNbO}_3$ there was an agreement only in respect of the real parts. The experimental dependences $I_s(\tau_1)$ obtained for this crystal were much narrower than those expected on the basis of the known polariton absorption coefficients α_p . Calculations based on the angular four-wave scattering spectra give values of α_p which differed by an order of magnitude (and sometimes more) from those obtained by other methods.

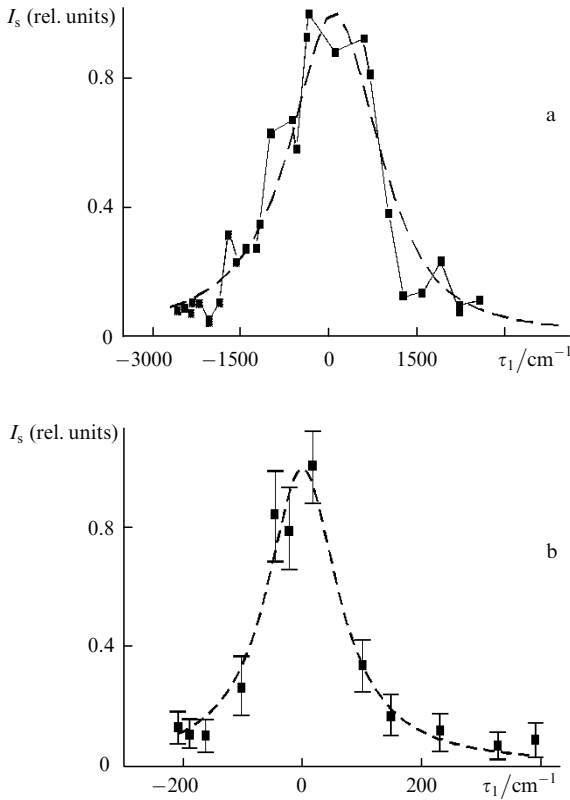


Figure 2. Dependences of the intensity I_s of a signal wave on the polarisation mismatch τ_1 in the case of LiIO_3 , characterised by $\alpha_p = 1300 \text{ cm}^{-1}$ (a) and for $\text{Mg}:\text{LiNbO}_3$, characterised by $\alpha_p = 50 \text{ cm}^{-1}$ (b). These values of α_p are approximate.

3. Four-wave scattering in crystals with a periodically poled structure

Our $\text{Mg}:\text{Nd}:\text{LiNbO}_3$ grown crystals were characterised by a periodic variation of the Nd impurity concentration and a periodic polydomain structure. The domain grating

had a period equal to the period of alternation of the growth layers (5.3 – 5.6 μm). Periodic variation of the direction of the vector representing the spontaneous polarisation P_s coincided with a change in the sign of the quadratic nonlinear susceptibility.

A spatial periodic variation of the quadratic nonlinearity $\chi_j^{(2)}(\mathbf{r})$ for each of the two stages of the cascade process (labelled by the subscripts $j = 1, 2$) gives rise to different Fourier harmonics:

$$\chi_j^{(2)}(\mathbf{r}) = \sum_{-\infty}^{\infty} \chi_{jm}^{(2)} \exp(im \mathbf{q} \cdot \mathbf{r}), \quad (10)$$

where

$$\chi_{jm}^{(2)} = \frac{1}{2\pi} \int_{-d/2}^{d/2} \chi_j^{(2)}(\mathbf{r}) \exp(-im \mathbf{q} \cdot \mathbf{r}) d\mathbf{r}; \quad (11)$$

m is an integer; $\mathbf{q} \equiv (2\pi/d)\mathbf{n}_z$ is the reciprocal superlattice vector; d is the domain structure period; \mathbf{n}_z is a unit vector directed along the normal to the growth layers.

We generalised the theory of four-wave scattering to the class of nonlinear periodically inhomogeneous crystals. When the scattering volume of a crystal is sufficiently large, so that condition (7) is satisfied, the distribution of the scattered-radiation intensity can be represented as follows:

$$I_s \propto \left| \left[\chi^{(3)} + \frac{4\pi\omega_p^2}{c^2} \frac{\chi_{10}^{(2)*} \chi_{20}^{(2)}}{|\mathbf{q}_{10}|^2 - (k'_p - ik''_p)^2} \right] f(\Delta\mathbf{k}_0) + \left[\sum_{m,n \neq 0} \frac{4\pi\omega_p^2}{c^2} \frac{\chi_{1n}^{(2)*} \chi_{2m}^{(2)}}{|\mathbf{q}_{1n}|^2 - (k'_p - ik''_p)^2} \right] f(\Delta\mathbf{k}_{n-m}) \right|^2, \quad (12)$$

where

$$\begin{aligned} \mathbf{q}_{1n} &\equiv \mathbf{k}_1 - \mathbf{k}_2 + n\mathbf{q}; \\ \mathbf{q}_{2m} &\equiv \mathbf{k}_L - \mathbf{k}_s + m\mathbf{q}; \\ \Delta\mathbf{k}_{n-m} &= \mathbf{q}_{2m} - \mathbf{q}_{1n}; \end{aligned} \quad (13)$$

$f(\mathbf{k})$ is a function which depends on the shape and dimensions of the scattering region:

$$f(\mathbf{k}) \equiv \int_V \exp(i\mathbf{k} \cdot \mathbf{r}) d\mathbf{r}. \quad (14)$$

For example, if the scattering region has the shape of a rectangular parallelepiped with the sides a , b , and c , we find that the function $f(\Delta\mathbf{k})$ becomes

$$f(\Delta\mathbf{k}) = V \frac{\sin(\Delta k_x a/2)}{\Delta k_x a/2} \frac{\sin(\Delta k_y b/2)}{\Delta k_y b/2} \frac{\sin(\Delta k_z c/2)}{\Delta k_z c/2}, \quad (15)$$

where Δk_x , Δk_y , Δk_z are the coordinates of the mismatch vector $\Delta\mathbf{k}$. If the region is a sphere of radius l , the function $f(\Delta\mathbf{k})$ depends only on Δk :

$$f(\Delta k) = 3V \frac{\sin(\Delta kl) - \Delta kl \cos(\Delta kl)}{(\Delta kl)^3}. \quad (16)$$

It is evident from expression (12) that the additional spatial harmonics of the functions $\chi_1^{(2)}$ and $\chi_2^{(2)}$ may give rise to additional maxima in the distribution of the signal radiation intensity. Moreover, if these maxima are suffi-

ciently wide, an additional interference pattern may be observed. Our experiments revealed additional maxima of the first and second orders of nonlinear diffraction [13]. The relationships between the intensities of the scattering into the various maxima were in good agreement with the available data on the profiles of the nonlinear superlattices of our crystals. As in the case of spatially homogeneous magnesium-doped LiNbO₃ crystals, the positions of the maxima agreed well with the theory, but their widths were considerably less than expected.

We cannot at present identify finally the cause of the discrepancy between the experimental results obtained by four-wave scattering in Mg : LiNbO₃ crystals and the theoretical predictions. However, we may assume that the observed line narrowing is associated with the weak photorefractive properties of the magnesium-doped LiNbO₃ crystals. There is no significant change in the refractive indices of these crystals under the influence of the powerful pump radiation, because the absence of such changes was confirmed by direct measurements (carried out by the method of least inclination of a prism) and was in agreement with the observation that the intensity maxima observed in four-wave scattering agreed with the predictions of the theoretical model. Nevertheless, there are evidently effects of a different type associated with the appearance of small-scale spatial inhomogeneities in crystals, which may distort the pump beams. As a result, the weak photorefractive properties may induce changes in the size and shape of the region where the pump waves intersect and the scattered radiation is generated. The condition of validity of the traditional model of scattering in a homogeneous layer, $l_{\alpha p} \gg 1$, may in this case be disobeyed.

4. Theory of four-wave scattering in spatially confined media

Further extension of the model of four-wave scattering to the case when the scattering region in a crystal is not too large compared with the mean free path of a polariton and is bounded along all three dimensions is desirable not only in the case of photorefractive crystals, but also for other types of inhomogeneous and low-dimensional structures.

Let us consider the four-wave cascade interaction in an arbitrary spatially confined region of a three-dimensional crystal. The dimensions of this region may be confined because the object itself has small dimensions or because the region in which the pump beams intersect is small. If the latter is true, we have to consider the following two volumes: V' , where the beams of the two 'heating' pumps intersect, and V'' , where a polariton interacts with the probe wave. In our calculations we shall use a phenomenological approach proposed by Klyshko [6] to describe four-wave scattering. This approach is based on the polariton Green function

$$G(k, \omega_p) = \frac{4\pi\omega_p^2/c^2}{k^2 \cos^2 \rho_p - (k'_p + ik''_p)^2} \quad (17)$$

(ρ_p is the anisotropy angle), which relates a plane wave of the quadratic nonlinear polarisation that appears in the first stage of the cascade process to a plane polariton wave which is excited by the former wave and which subsequently interacts with the probe wave in the second stage of the cascade scattering process. In a spatially confined medium

the nonlinear polarisation waves are not plane and the Green polariton function described by the above expression relates the separate Fourier components of the polarisation and of the polariton field. In our calculations we shall take into account the spatial dependences of the quadratic polarisation amplitudes in the direct processes; this will be done in the simplest possible form. The nonlinear polarisation waves are regarded as plane inside the scattering region, whereas outside this region their amplitudes are assumed to be zero. Within the framework of this approximation any change in the pump wave amplitudes can be regarded as negligible within the beam cross sections.

The resultant field of a polariton wave and of a scattered-radiation wave is determined by integration over all the Fourier components. The general expression for the scattered-radiation intensity, considered as a function of the phase mismatch, is

$$I_s \propto \left| \chi^{(3)} f''(\Delta k) + \frac{\chi_1^{(2)*} \chi_2^{(2)}}{(2\pi)^2} \int G^*(k, \omega_p) \times f'^*(q_1 - k) f''(q_2 - k) dk \right|^2, \quad (18)$$

where

$$\begin{aligned} q_1 &\equiv k_1 - k_2; \\ q_2 &\equiv k_L - k_s; \\ \Delta k &\equiv q_2 - q_1. \end{aligned} \quad (19)$$

The functions $f'(q_1 - k)$ and $f''(q_2 - k)$ depend on the geometry of the scattering regions and are calculated, in accordance with expression (14), by integration over the volumes V' and V'' . If the linear dimensions of the scattering regions are much greater than the mean free path of a polariton, we obtain the same expression for I_s as that reported in earlier investigations. However, when the dimensions of these regions are reduced, the dependence of the intensity on the polariton mismatch becomes sensitive to the actual shape and size of the regions V' and V'' .

Acknowledgements. This work was supported by the Russian Foundation for Basic Research (Grants Nos 96-02-16336a and 98-02-16877).

References

1. Polivanov Yu N *Usp. Fiz. Nauk* **126** 185 (1978) [*Sov. Phys. Usp.* **21** 805 (1978)]
2. Coffinet J P, DeMartini F *Phys. Rev. Lett.* **22** 60 (1969)
3. Yablonovitch E, Flytzanis C, Bloembergen N *Phys. Rev. Lett.* **29** 865 (1972)
4. Wynne J J *Phys. Rev. Lett.* **29** 650 (1972)
5. Polivanov Yu N, Sukhodol'skii A T *Pis'ma Zh. Eksp. Teor. Fiz.* **25** 240 (1977) [*JETP Lett.* **25** 221 (1977)]
6. Klyshko D N *Kvantovaya Elektron. (Moscow)* **2** 265 (1975) [*Sov. J. Quantum Electron.* **5** 149 (1975)]
7. Strizhevskii V L, Yashkir Yu N *Kvantovaya Elektron. (Moscow)* **2** 995 (1975) [*Sov. J. Quantum Electron.* **5** 541 (1975)]
8. Vallee F, Flytzanis C *Phys. Rev. B* **46** 13799 (1992); *Phys. Rev. Lett.* **74** 3281 (1995)
9. Qiu T, Maier M *Phys. Rev. B* **56** R5717 (1997)
10. Kitaeva G Kh, Mikhailovsky A A, Losevsky P S, Penin A N *Opt. Commun.* **138** 242 (1997)

11. Burlakov A V, Chekhova M V, Kulik S P, Penin A N *Technical Digest of the Pacific Rim Conference on Lasers and Electro-Optics (CLEO/Pacific Rim '97), Chiba, Japan, 1997* (New York: Institute of Electrical and Electronics Engineers, 1997) p. 102
12. Nikogosyan D N *Kvantovaya Elektron. (Moscow)* **4** 5 (1977) [*Sov. J. Quantum Electron.* **7** 1 (1977)]
13. Kitaeva G Kh, Mikhailovskii A A, Penin A N *Zh. Eksp. Teor. Fiz.* **112** 2001 (1997) [*J. Exp. Theor. Phys.* **85** 241 (1997)]